International Journal of Pharmaceutics 660 (2024) 124299

Contents lists available at ScienceDirect

International Journal of Pharmaceutics

journal homepage: www.elsevier.com/locate/ijpharm

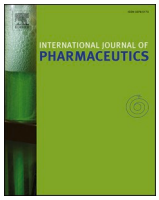

3D printed dispersible efavirenz tablets: A strategy for nasogastric administration in children

Nadine Lysyk Funk [a,b,c], Patricija Januskaite [c], Ruy Carlos Ruver Beck [a,b], Abdul W. Basit [c,d,e,*], Alvaro Goyanes [c,d,e,f,**]

[a] Programa de Pós-Graduação em Ciências Farmacêuticas, Faculdade de Farmácia, Universidade Federal do Rio Grande do Sul, Porto Alegre, Brazil
[b] Laboratório de Nanocarreadores e Impressão 3D em Tecnologia Farmacêutica (Nano3D), Faculdade de Farmácia, Universidade Federal do Rio Grande do Sul (UFRGS), Porto Alegre, Brazil
[c] Department of Pharmaceutics, UCL School of Pharmacy, University College London, 29-39 Brunswick Square, London WC1N 1AX, UK
[d] FABRX Ltd., Henwood House, Henwood, Ashford, Kent TN24 8DH, UK
[e] FABRX Artificial Intelligence, Carretera de Escairón, 14, Currelos (O Saviñao) CP 27543, Spain
[f] Departamento de Farmacología, Farmacia y Tecnología Farmacéutica, I+D Farma (GI-1645), Facultad de Farmacia, Instituto de Materiales (iMATUS) and Health Research Institute of Santiago de Compostela (IDIS), Universidade de Santiago de Compostela, 15782 Santiago de Compostela, Spain

ARTICLE INFO

Keywords:
Additive manufacturing of oral drug products
Enteral route administration of medicines
Nasogastric tubes and ostomies
Printed formulations and drug delivery systems
Powder bed fusion 3D printing pharmaceuticals
Pediatrics and acceptability

ABSTRACT

Enteral feeding tubes (EFTs) can be placed in children diagnosed with HIV which need nutritional support due to malnutrition. EFTs are the main route for medication administration in these patients, bringing up concerns about off label use of medicines, dose inaccuracy and tube clogging. Here we report for the first time the use of selective laser sintering (SLS) 3D printing to develop efavirenz (EFZ) dispersible printlets for patients with HIV that require EFT administration. Water soluble polymers Parteck® MXP and Kollidon® VA64 were used to obtain both 500 mg (P500 and K500) and 1000 mg printlets (P1000 and K1000) containing 200 mg of EFZ each. The use of SLS 3D printing obtained porous dosage forms with high drug content (20 % and 40 % w/w) and drug amorphization using both polymers. P500, K500 and K1000 printlets reached disintegration in under 230 s in 20 mL of water (25 ± 1 °C), whilst P1000 only partially disintegrated, possibly due to saturation of the polymer in the medium. As a result, the development of dispersible EFZ printlets using hydrophilic polymers can be explored as a potential strategy for drug delivery through EFTs in paediatrics with HIV, paving the way towards the exploration of more rapidly disintegrating polymers and excipients for SLS 3D printing.

1. Introduction

Human immunodeficiency virus (HIV) has been a public health concern since its recognition in 1981. Worldwide, about 39 million people were living with HIV in 2022, among which 1.5 million were children aged 0–14 years (WHO, 2023). Pharmacological treatment in HIV-positive children can include efavirenz (EFZ), a specific, non-nucleoside reverse transcriptase inhibitor, with daily doses varying from 100 to 600 mg, given once or three times a day, according to the age and stage of treatment (Sustiva, 2023; WHO, 2019).

HIV is especially aggressive in children, as up to 71.8 % of HIV-positive infants can also present severe acute malnutrition that plays an important role in disease progression (Abate et al., 2020; Rose et al., 2014). The enteral route can be an alternative to nutritional supplementation in HIV-positive patients to promote body weight recovery and reduce chronic inflammation, benefiting overall treatment (Geng et al., 2021). For that purpose, enteral feeding tubes (EFTs) can be placed in patients through the nasopharynges or through the skin, as gastrostomies and jejunostomies (FDA, 2021). Although mainly aimed for nutritional supplementation, the enteral route often becomes the main route of medicine administration, raising concerns about the off-label use of medicines that can lead to tube clogging, dose inaccuracy, and may compromise the safety and efficacy of pharmacological treatments (Blaszczyk et al., 2023).

When pursuing alternatives to overcome the challenges presented by drug delivery through EFTs, the development of soluble tablets to be

* Corresponding author at: Department of Pharmaceutics, UCL School of Pharmacy, University College London, 29-39 Brunswick Square, London WC1N 1AX, UK.
** Corresponding author at: Department of Pharmaceutics, UCL School of Pharmacy, University College London, 29-39 Brunswick Square, London WC1N 1AX, UK.
E-mail addresses: a.basit@ucl.ac.uk (A.W. Basit), a.goyanes@fabrx.co.uk (A. Goyanes).

https://doi.org/10.1016/j.ijpharm.2024.124299
Received 19 April 2024; Received in revised form 29 May 2024; Accepted 31 May 2024
Available online 2 June 2024

disintegrated and/or dissolved in a small amount of liquid prior to administration should be considered. In this scenario, three-dimensional (3D) printing (3DP) can be a powerful tool to obtain solid dosage forms with specific release or disintegration profiles (de Oliveira et al., 2022; Suárez-González et al., 2021; Tranová et al., 2022; Trenfield et al., 2023), also enabling dose adjustment during treatment according to patient needs (dos Santos et al., 2023; Rodríguez-Pombo et al., 2024; Seoane-Viaño et al., 2023; Windolf et al., 2022). Up to now, 3DP dosage forms feasible for EFT delivery have been developed by semi-solid extrusion using cellulose-based polymers: 0.1–2 mg warfarin films (Panraksa et al., 2021) and 75 mg phenytoin sodium tablets (Öblom et al., 2019).

Among the 3DP techniques, selective laser sintering (SLS) consists of a powder bed technique using a laser to bind the powder particles together and build up the desired dosage form (Abdalla et al., 2023; Kayalar et al., 2024; Seoane-Viaño et al., 2024; Tabriz et al., 2023). The laser speed can be modified to obtain printlets with higher porosity (Trenfield et al., 2023) and accelerated disintegration and/or dissolution such as orally disintegrating tablets (Allahham et al., 2020; Fina et al., 2018b; Khuroo et al., 2022). Moreover, with SLS it is feasible to achieve a high drug loading by incorporating up to 80 % (w/w) of drug in the printing formulation (Kulinowski et al., 2022).

The main polymeric excipient plays an important role for a medicine to achieve a fast disintegration and/or dissolution. Hydrophilic polymers such as Kollidon® VA 64 (Allahham et al., 2020; Awad et al., 2020b; Fina et al., 2018b), Kollicoat® IR (Khuroo et al., 2022) and hydroxypropylmethylcellulose (HPMC) (Madžarević et al., 2021) have been reported in the development of SLS printlets presenting disintegration of up to 30 s or an immediate release profile. However, is worth noticing that the described studies encompass small dosage forms with weight varying from 5 to 230 mg, containing up to 10 mg of drug per printlet.

To expand the possibilities of polymeric matrices with fast disintegration and/or dissolution properties, our work explored the use of Parteck® MXP as the main excipient for SLS formulations, along with Kollidon® VA64 (Copovidone), a well-established fast-disintegrating polymer that has been used in SLS systems successfully (Allahham et al., 2020; Fina et al., 2018b; Gueche et al., 2021a; Tabriz et al., 2023; Thakkar et al., 2021b, 2021a). Parteck® MXP is a polyvinyl alcohol especially designed for hot-melt extrusion, affording the incorporation of high drug loadings and improving solubilization and stability of drugs (Merck, 2023). Its use has been described in the development of modified-release (Windolf et al., 2022) and immediate-release (Crișan et al., 2022) 3D printed medicines developed by fused deposition modelling and controlled-release dosage forms produced by SLS (Tikhomirov et al., 2023).

Recognizing the growing interest in the development of dosage forms feasible for EFT, this study aims to develop printlets containing 200 mg of EFZ by SLS 3DP to be disintegrated and/or dissolved prior to enteral administration. Additionally, we investigate the influence of polymer choice (Parteck® MXP and Kollidon® VA64) and dosage form size on the printlet disintegration time.

2. Materials and methods

2.1. Materials

The polymer Parteck® MXP 4–88 (polyvinyl alcohol, hydrolysis grade of 88 %, Mw 32,000 g/mol) was kindly donated by Merck (Darmstadt, Germany) and Kollidon® VA64 (copolymer of N-vinylpyrrolidone and vinyl acetate – molar ratio of 6:4, Mw 45,000 – 70,000 g/mol) acquired from Basf (Ludwigshafen, Germany). The colorant Candurin® Gold Sheen was purchased from Merck (Darmstadt, Germany) and the drug efavirenz from Zhejiang Jiangbei Pharmaceutical Co., Ltd. (Zhejiang, China).

2.2. Pharma-ink preparation

Pharma-inks were prepared by mixing the excipients and drug using a pestle and mortar according to the composition described in Table 1. They were developed with a higher (77 % w/w) and lower (57 % w/w) polymer concentration to observe its influence on disintegration time, and the total printlet weight was designed to achieve 200 mg of drug per dosage form. To ensure printability, Candurin® Gold Sheen was added to all formulations as a laser absorbent. After mixing, the formulations were sieved (180 μm pore diameter) to ensure particle size homogeneity and proper powder flowability.

2.3. SLS 3D printing

Cylindrical tablets were designed using PrusaSlicer 2.5.2 software with the dimensions to obtain dosage forms with 200 mg of EFZ, as described in Table 2. The stl. file was exported to Sintratec Central 1.1.13 and printlets were obtained with the Sintratec Kit (AG, Brugg, Switzerland) SLS 3D printer, equipped with a 2.3 W blue diode laser (445 nm) and reservoir platform and building platform of 150 mm × 150 mm × 150 mm. The printing temperature and laser speed were adjusted according to each polymer glass transition temperature (Kollidon® VA64, 101 °C; Parteck® MXP, 160–240 °C) (Basf, 2022; Merck, 2023), to guarantee proper fusion of the particles and, thus, a strong dosage form.

2.4. Thermal analysis

The thermal behaviour of raw materials, pharma-inks and printlets were evaluated using differential scanning calorimetry (DSC) and thermogravimetric analysis (TGA). DSC measurements were made with a Q2000 DSC (TA Instruments, Waters, LLC, USA), using a nitrogen flow of 50 mL/min and a temperature rate of 10 °C/min up to 200 °C. TGA analysis was performed using a Discovery TGA (TA instruments, Waters, LLC, USA), with a heating rate of 10 °C/min up to 300 °C and a nitrogen flow rate of 25 mL/min.

2.5. X-ray powder diffraction (XRPD)

Formulations were prepared (Table 1) and discs of 23 mm diameter × 1 mm height were printed and analysed along with the bulk materials (EFZ, Parteck® MXP and Kollidon® VA64) and pharma-inks. Rigaku Miniflex 600 (Rigaku, Texas, USA) equipment was used to obtain the X-ray diffraction patterns of samples (Cu K X-ray source, = 1.5418 A) applying an intensity of 15 mA and voltage of 40 kV. An angular range from 3 to 50° was employed with a stepwise size of 0.02° and speed of 5 °/min.

2.6. Printlet characterization

2.6.1. Morphology

The diameter and height of the printlets were measured using a digital calliper (DigiMax®, Dublin, Ireland) and their weight using a FisherBrand analytical balance (Fisher Scientific, Leicestershire, UK) (n = 10). The mean was calculated, and the results were expressed as mean ± standard deviation.

2.6.2. Scanning electronic microscopy (SEM)

The morphology of EFZ printlets was observed using a JSM-840A Scanning Microscope (JEOL GmbH, Freising, Germany). Prior to the analysis, the printlets were placed on a self-adhesive carbon disc, mounted onto a 25 mm aluminium stub, and coated with 25 nm of gold using a sputter coater. Images of the surface (280×) and internal structures (420×) were acquired at a 10 kV accelerated voltage.

Table 1
Composition of the pharma-inks used to obtain the SLS printlets. All formulations contained 200 mg of EFZ.

Formulation code	EFZ (% w/w)	Parteck® MXP (% w/w)	Kollidon® VA64 (% w/w)	Candurin® Gold Sheen (% w/w)	Theoretical weight (mg)
P500	40	57	–	3	500
P1000	20	77	–	3	1000
K500	40	–	57	3	500
K1000	20	–	77	3	1000

Table 2
Printing parameters and theoretical printlet dimensions.

Formulation code	Surface temperature (°C)	Chamber temperature (°C)	Laser speed (mm/s)	Width (mm)	Height (mm)
P500	120	100	75	20	5.5
P1000	120	100	75	22	9.3
K500	100	80	100	20	5.5
K1000	100	80	100	20	8.8

2.6.3. Disintegration testing

The time required for the printlets to disintegrate was evaluated mimicking usual practices for medicines administration through the enteral route. Disintegration time was measured adding tablets to a beaker containing 20 mL of water, at 26 ± 2 °C and constant stirring (1500 rpm). The endpoint of the disintegration was recorded when the printlet integrity was no longer visualized, and only small particles could be observed.

2.6.4. Drug content

For drug quantification, tablets were crushed and diluted in a mixture of methanol and water. First, 10 mL of water was added to a 25 mL volumetric flask containing the crushed printlet and the mixture was stirred for 10 min at 1500 rpm to guarantee polymer solubilization. The volumetric flask was then filled with methanol and stirred for 20 min (1500 rpm) for drug solubilization. Samples were diluted (20 μg/mL), filtered (0.45 μm filter) (Sigma Aldrich, UK) and analysed by high-performance liquid chromatography (HPLC) (Agilent 1290 Infinity II, Agilent Technologies, UK), equipped with a 1290 Infinity II variable UV wavelength detector.

A Zorbax Eclipse C18 column (4.6 mm × 150 mm, 5 μm) was employed at a constant temperature of 35 °C, and the mobile phase consisted of a mixture of acetonitrile (70 %) and water (30 %) at a flow rate of 1 mL/min. The injection volume was 20 μL and efavirenz was detected in 4.5 min at 247 nm. The method was made in the concentration range of 1–80 μg/mL, with a detection limit of 0.324 μg/mL and quantification limit of 0.982 μg/mL.

2.6.5. Statistical analysis

All data were presented as mean ± standard deviation (SD). Statistical analysis was carried out by Student's *t* test or one-way ANOVA followed by Tukey's *post-hoc* test, at a significance level of 5 % (GraphPad Prism 5.0, GraphPad software, Inc., USA).

3. Results and discussion

Formulation optimization was conducted by adjusting the polymer and drug ratio to obtain a pharma-ink with suitable flowability. Powder formulations were sieved before printing, as a homogeneous particle size distribution is consider crucial for a proper powder flow and a homogenous sintering during printing (Awad et al., 2020a). As shown in previous studies, the colorant Candurin® Gold Sheen was added at a fixed concentration of 3 % w/w to enhance laser absorption and allow a proper degree of sintering (Fina et al., 2018a; Trenfield et al., 2020). Candurin® Gold Sheen is a mica-based colorant, considered safe for oral administration and accepted for pharmaceutical use, being widely employed in tablet coatings, food applications, and used as a colorant (FDA, 2024; Merck, 2023). The dimensions were adjusted to reach the desired printlet weight, resulting in dosage forms containing 200 mg of EFZ each (Fig. 1a).

Formulations containing 20 % (w/w) and 40 % (w/w) of EFZ demonstrated suitable powder flowability using both Parteck® MXP and Kollidon® VA64, enabling the successful manufacture of 1000 mg and 500 mg SLS printlets (Fig. 1b). Differences in height and width were observed between Parteck® MXP and Kollidon® VA64 printlets of 1000 mg, which can be explained by the difference in the molecular weight of the polymers (34,000 g/mol and 40,000 – 75,000 g/mol, respectively) (Basf, 2022; Merck, 2022) that are present in a higher amount in these formulations (57 % w/w).

EFZ printlets presented variability in width and height compared to the designed 3D model, as shown in Table 3. Physical modifications can be expected during SLS printing due to particle partial melting that may lead to densification and volume shrinking (Kulinowski et al., 2021; Mokrane et al., 2018). Despite the variations observed in width and height, all four dosage forms displayed weight and drug content close to the theoretical values (Table 3). P500 and P1000 printlets presented a mean weight of 505.4 ± 8.5 mg and 1002.3 ± 6.6 mg, respectively, and K500 and K1000 of 502.0 ± 6.5 mg and 1016.3 ± 9.7, respectively. The percentage deviation of weight observed was within the ± 5 % range described by the United States Pharmacopoeia for tablets with an average mass higher than 250 mg (USP, 2022).

SEM images (Fig. 2) showed a proper sintering of powder particles after the printing process and confimed a porous surface and interior of printlets. The presence of channels along the structure can facilitate medium entrance and interaction within the printlets and potentially accelerate dosage form disintegration. Both Parteck printlet interiors (P500 and P1000) exhibited fibre-like structures between the particles, which may affect the disintegration profile of the structure as a result of stronger bond presence.

To ensure EFZ and excipient stability and prevent degradation during the printing process, thermal behaviour of bulk materials was evaluated using TGA. The polymers Parteck® MXP and Kollidon® VA64

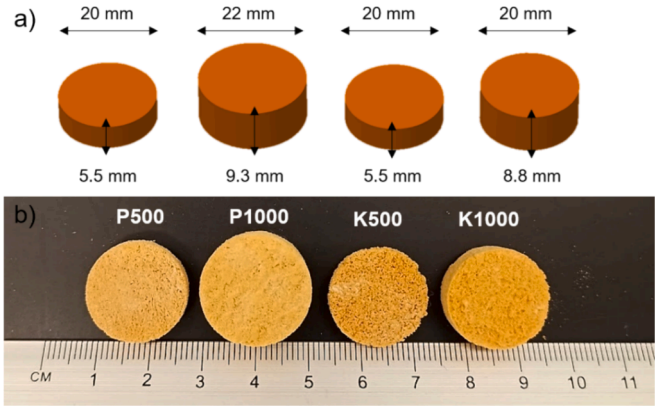

Fig. 1. a) stl. files and theoretical dimensions of the printlets and b) image of EFZ printlets (500 and 1000 mg) printed from Parteck® MXP (P500 and P1000) and Kollidon® VA64 (K500 and K1000). Scale is in cm.

Table 3
Physical characterization and drug content (n = 4) of EFZ printlets.

Formulation code	Weight (mg ± SD)	Width (mm ± SD)	Height (mm ± SD)	Drug content (mg/printlet)
P500	505.4 ± 8.5	18.7 ± 0.2	5.1 ± 0.1	505.4 ± 8.5
P1000	1000.0 ± 6.6	20.2 ± 0.1	8.9 ± 0.3	1002.3 ± 6.6
K500	505.2 ± 7.2	18.4 ± 0.1	4.7 ± 0.1	502.0 ± 6.5
K1000	1016.3 ± 9.7	18.5 ± 0.1	8.8 ± 0.1	1016.3 ± 9.7

presented ~ 3.5 % and ~ 5.9 % weight loss at 100 °C, respectively, which can be attributed to water evaporation (Fig. 3). No significant weight loss was observed for Parteck® MXP from 100 °C to 120 °C, which was the chosen printing temperature range. The degradation onset of both polymers occurred at around 225 °C and 270 °C for Parteck® MXP and Kollidon® VA64, respectively, which is in agreement with previous reports (Tabriz et al., 2023; Merck, 2016). EFZ presented its complete degradation from 160 °C, below the printing temperature used in this study. Along with the light brown colour visualized after the printing process, TGA thermograms confirmed that all the components were thermally stable in the temperature employed for SLS printing.

DSC thermograms showed an EFZ endothermic peak at 139.3 °C, which is characteristic of its melting point (Fig. 4)(Seoane-Viaño et al., 2023). DSC data suggested drug amorphization within all the printlets and after the physical mixture of Kollidon® VA64 and EFZ (K500 and K1000). The absence of drug crystallinity in the DSC thermogram for Kollidon® VA64 powders can be attributed to the possible dissolution of EFZ particles within the polymer structure because of heating during analysis. This phenomena can be facilitated in small particles due to their increased surface area (Dedroog et al., 2020). On the other hand, traces of crystalline EFZ were observed for Parteck® MXP pharma-ink formulations. Although less intense than the bulk EFZ, a higher intensity was displayed for P500 in comparison to the P1000 due to the higher drug loading (40 % w/w vs 20 % w/w).

To further investigate the EFZ form within the pharma-inks and printlets, XRPD analysis was performed. Diffractograms exhibited the characteristic pattern of crystalline EFZ with a sharp and intense Bragg peak at 2θ of 6.06° followed by medium intensity peaks at 14.1°, 20.02°, 21.14° and 24.7°, which have been observed by other authors (Ngilirabanga et al., 2020) (Fig. 5).

The EFZ crystalline pattern was also observed in the pharma-inks, regardless of the polymer used. Peak intensity at 6.06° was higher in

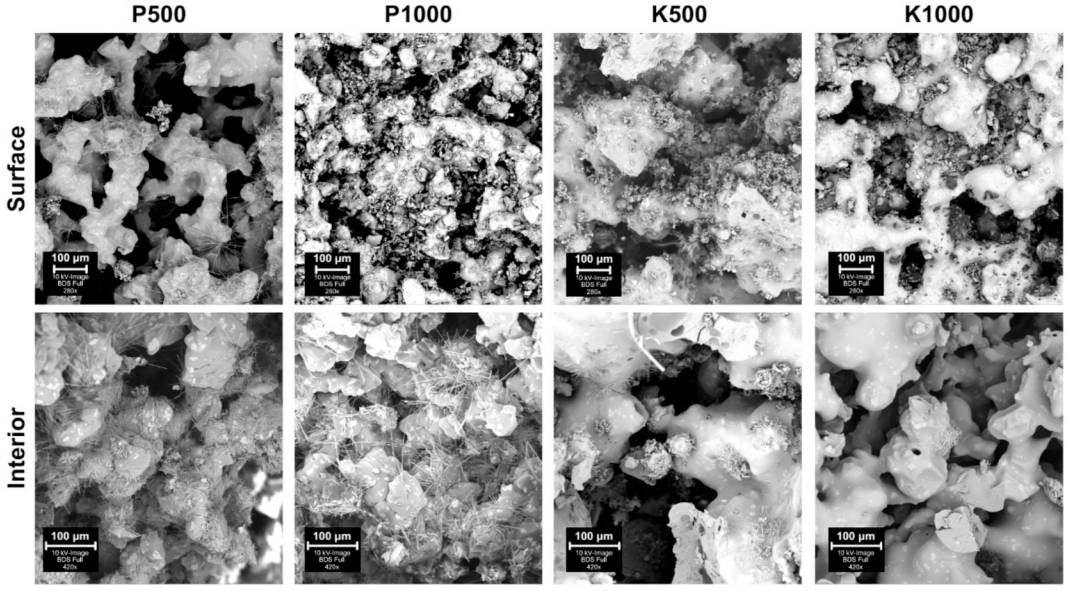

Fig. 2. SEM images of surface (280×) and interior (420×) of EFZ printlets.

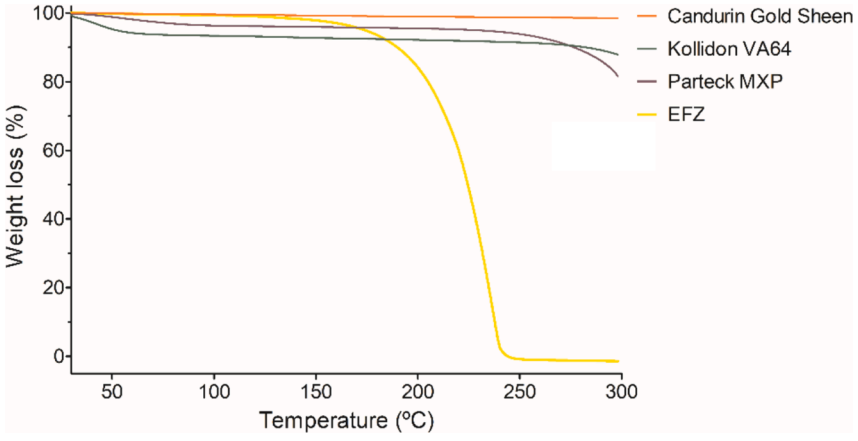

Fig. 3. TGA results of raw materials in the formulations: EFZ, Parteck® MXP, Kollidon® VA64, and Candurin® Gold Sheen.

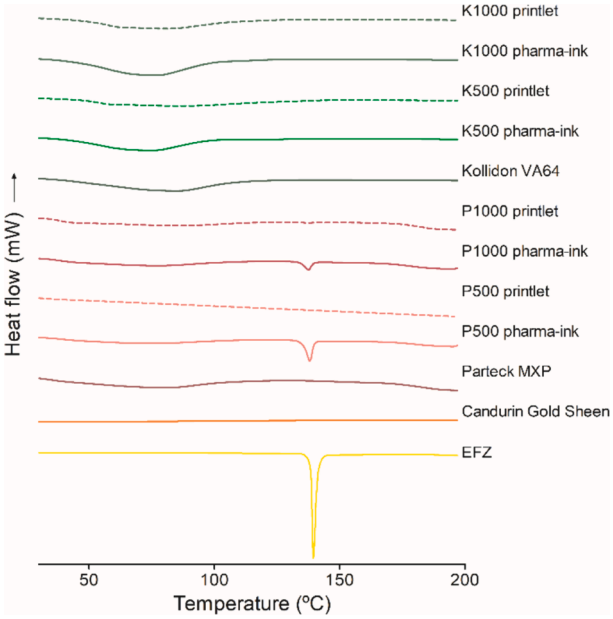

Fig. 4. DSC thermograms of pure drug (EFZ), excipients (Candurin® Gold Sheen, Parteck® MXP and Kollidon® VA64) and SLS formulations prior (pharma-ink) and after (printlets) printing.

P500 and K500 in comparison to P1000 and K1000, due to differences in drug loading (40 % and 20 % w/w, respectively). Although being less sensitive than DSC (de Oliveira et al., 2023; Thakral et al., 2018), XRPD analysis was able to detect drug crystals within the four pharma-inks as no heating took place unlike in the DSC. On the other hand, corroborating with the DSC results, the absence of the EFZ crystalline patterns in XRPD diffractograms suggested drug amorphization after the printing process for all four formulations, a phenomena previously described in literature as a result of SLS printing (Kayalar et al., 2024; Madžarević et al., 2021).

A disintegration assay was performed to mimic usual practices for EFT administration of medicines. According to the Handbook of Drug Administration via Enteral Feeding Tubes (White and Bradnam, 2015), prior to administration medicines can be dispersed in small volumes of water ranging from 10 to 30 mL for EFT delivery, to avoid side effects in patients such as nausea and vomiting. Therefore, the printlet disintegration assay was conducted in a beaker containing 20 mL of water (Fig. 6). Disintegration end point was recorded as the time when printlet integrity was not observed and only small particles could be visualized.

Literature has shown that physical characteristics of printlets developed by SLS can be modulated by changing the laser speed or polymer nature (Gueche et al., 2021b; Lupone et al., 2022; Tikhomirov et al., 2023). Slower printing speeds have the potential to increase powder particle sintering, resulting in more dense structures with less porosity that can make it difficult for solvent entrance and interaction with the printlet interior, slowing down disintegration and dissolution of SLS dosage forms (Fina et al., 2018b; Thakkar et al., 2021b).

In the present study, Parteck® MXP formulations (P500 and P1000) were printed at a slower printing speed (75 mm/s) than Kollidon® VA64 formulations (100 mm/s). As previously mentioned, changes in the printing speed were necessary to obtain a strong dosage form for each polymer. Regardless of the printing speed employed, results showed that disintegration of P500, K500 and K1000 printlets occurred in less than 230 s, with the P1000 formulation only partially disintegrating (>2700 s), as shown in Table 4. No significant statistical differences ($p < 0.05$) were reported for the disintegration times of P500, K500, and K1000. Moreover, P500 and K500 printlets meet European Pharmacopeia requirements for dispersible tablets, disintegrating within 3 min (EuPh, 2019).

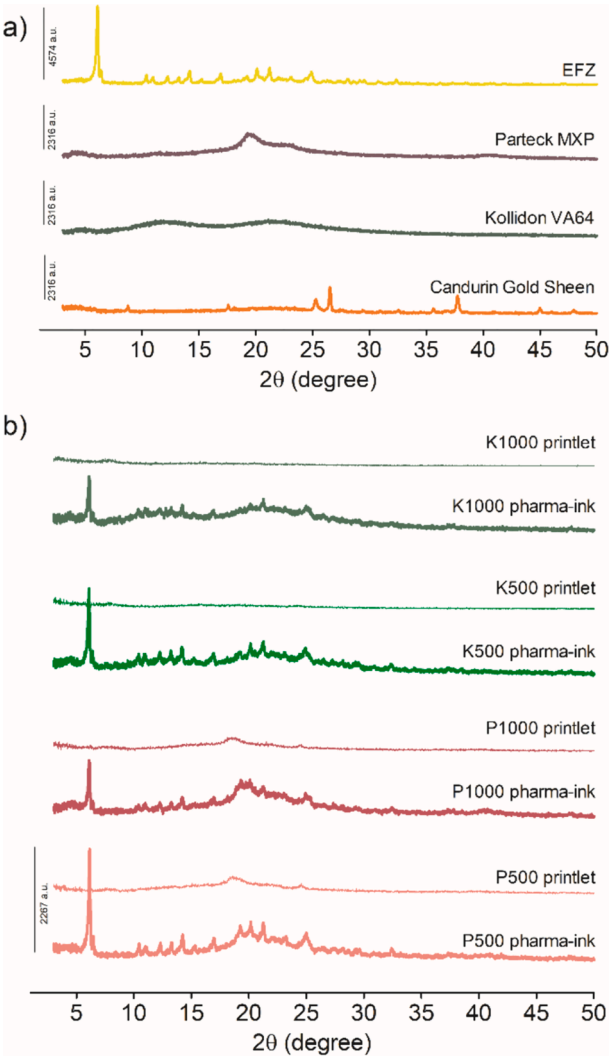

Fig. 5. X-ray diffractograms of a) pure excipients and b) EFZ formulations before (pharma-ink) and after (printlets) the printing process. Scale bars in Y axes represent maximum peak intensity.

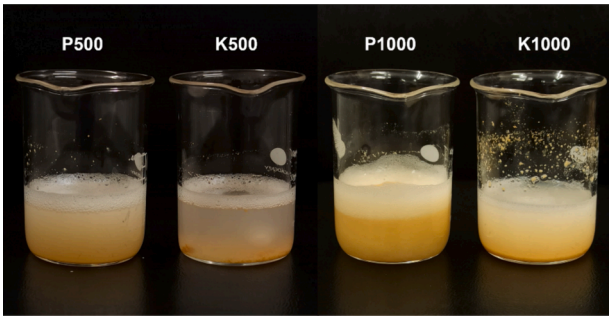

Fig. 6. Illustration of P500, K500 and K1000 after its disintegration assay endpoint. P1000 did not completely disintegrate so the experiment was stopped at 45 mins.

P1000 printlets were weighed after 45 min and approximately 42 ± 5 % w/w of the initial dosage form remained intact. The incomplete solubilization of Parteck® MXP particles in the disintegration media may be explained by saturation of the polymer due to the small amount of water employed in the assay, not allowing the printlet to fully solubilize in the disintegration media. Although polymer solubilization is a

Table 4
Calculation of the surface area (SA), volume (V) and SA:V ratio; and disintegration time (n = 3) of Parteck® MXP and Kollidon® VA64 printlets. No statistically significant difference observed in disintegration time ($p < 0.05$).

Formulation code	Surface area (mm^2)	Volume (mm^3)	SA:V ratio (mm^{-1})	Disintegration time (s)
P500	854.9 ± 17	1422.3 ± 41	0.60 ± 0.01	148 ± 112
P1000	1202.3 ± 23	2828.4 ± 107	0.43 ± 0.01	>2700
K500	804.3 ± 13	1250.6 ± 43	0.64 ± 0.01	111 ± 11
K1000	1042.5 ± 9	2342.1 ± 30	0.45 ± 0.01	199 ± 28

desirable characteristic, using a greater amount of water to enable complete P1000 solubilization may result in patient side effects such as nausea and vomiting, presenting a challenge for the enteral administration of this dosage form.

Overall, all four printlets showed statistically significant ($p < 0.05$) differences in surface area to volume (SA/V) ratio (K500 > P500 > K1000 > P1000), with a higher ratio found for the 500 mg printlets (0.60 and 0.64 mm^{-1} for P500 and K500, respectively) in comparison to the 1000 mg printlets (0.43 and 0.45 mm^{-1} for P1000 and K1000, respectively), as expected for objects with different dimensions and the same geometry (dos Santos et al., 2023; El Aita et al., 2020). Studies have reported the importance of SA:V ratio to understand the solvent interaction with pharmaceutical dosage forms which impacts disintegration time and drug release (Fina et al., 2018a). Interestingly, it was possible to observe a statistical similarity in the disintegration time for P500, K500, and K1000 regardless of the differences observed in the SA:V ratio. This outcome may suggest an outstanding role of polymer characteristics on disintegration phenomena.

As already discussed, a decisive factor for disintegration of pharmaceutical dosage forms is solvent penetration through the printlet pores, also known as capillary action or wicking (Berardi et al., 2021). Porous structures result in a rapid solvent entrance into the printlet core, resulting in a one-step disintegration process, as seen in the present study for the Kollidon® VA64 formulations. On the other hand, a slow solvent penetration can also occur and promote a gradual disintegration by polymeric erosion from the outer layer to the core. This process can describe the disintegration of the Parteck® MXP printlets and justify the partial disintegration of P1000 (Berardi et al., 2021; Funk et al., 2022).

Distinctive disintegration phenomena observed between Parteck® MXP and Kollidon® VA64 printlets showed that each polymer characteristic can provide a different strategy to achieve a dispersible dosage form. Overall, results demonstrated the potential of SLS 3DP to personalize dosage forms for enteral administration as an alternative from conventional dosage forms, offering customizable printlets in dose, size, and disintegration time. Further research into excipients could amplify applications of water-soluble polymers in SLS 3DP, ensuring both patient safety and caregiver comfort during drug delivery via nasogastric tubes.

4. Conclusion

This study showed for the first time the use of SLS 3D printing for the development of dispersible EFZ printlets intended for enteral administration. Printlets of 500 mg and 1000 mg weight and containing 200 mg of drug each were successfully manufactured with two water-soluble polymers: Parteck® MXP and Kollidon®[e] VA64. SLS 3D printing enabled the production of porous printlet structures and amorphous conversion of EFZ regardless of the formulation. Similar disintegration times were found for P500, K500 and K1000 (<230 s), with only partial disintegration for P1000. It was found that Parteck® MXP may be used for rapidly disintegrating formulations for small size dosage forms, but more polymers must be investigated to expand the application of SLS 3DP for enteral route administration.

CRediT authorship contribution statement

Nadine Lysyk Funk: Writing – review & editing, Writing – original draft, Methodology, Investigation, Funding acquisition, Formal analysis, Data curation, Conceptualization. **Patricija Januskaite:** Writing – review & editing, Visualization, Validation, Resources, Project administration, Funding acquisition. **Ruy Carlos Ruver Beck:** Visualization, Validation, Supervision, Project administration, Funding acquisition, Conceptualization. **Abdul W. Basit:** Writing – review & editing, Validation, Supervision, Resources, Project administration. **Alvaro Goyanes:** Writing – review & editing, Visualization, Validation, Supervision, Resources, Project administration, Formal analysis, Conceptualization.

Declaration of competing interest

The authors declare the following financial interests/personal relationships which may be considered as potential competing interests: Abdul W. Basit reports a relationship with FABRX Ltd. that includes: employment and equity or stocks. Alvaro Goyanes reports a relationship with FABRX Ltd. that includes: employment and equity or stocks. If there are other authors, they declare that they have no known competing financial interests or personal relationships that could have appeared to influence the work reported in this paper.

Data availability

Data will be made available on request.

Acknowledgments

This study is part of the National Institute of Science and Technology in 3D printing and Advanced Materials Applied to Human and Veterinary Health - INCT_3D-Saúde, funded by CNPq/Brazil (Grant #406436/2022-3). N. L. Funk thanks CAPES (Finance Code 001) and the National Council for Scientific and Technological Development – CNPq/Brazil (200172/2023-9) for her PhD fellowships. This research was partially funded by the Engineering and Physical Sciences Research Council (EPSRC) UK, grant number EP/S023054/1 and by Xunta de Galicia [ED431C 2024/09].

References

Abate, B.B., Aragie, T.G., Tesfaw, G., 2020. Magnitude of underweight, wasting and stunting among HIV positive children in East Africa: A systematic review and meta-analysis. PLoS One 15, 1–22. https://doi.org/10.1371/journal.pone.0238403.

Abdalla, Y., Elbadawi, M., Ji, M., Alkahtani, M., Awad, A., Orlu, M., Gaisford, S., Basit, A. W., 2023. Machine learning using multi-modal data predicts the production of selective laser sintered 3D printed drug products. Int. J. Pharm. 633 https://doi.org/10.1016/j.ijpharm.2023.122628.

Allahham, N., Fina, F., Marcuta, C., Kraschew, L., Mohr, W., Gaisford, S., Basit, A.W., Goyanes, A., 2020. Selective laser sintering 3D printing of orally disintegrating printlets containing ondansetron. Pharmaceutics 12, 1–13. https://doi.org/10.3390/pharmaceutics12020110.

Awad, A., Fina, F., Goyanes, A., Gaisford, S., Basit, A.W., 2020a. 3D printing: Principles and pharmaceutical applications of selective laser sintering. Int. J. Pharm. 586, 29–39. https://doi.org/10.1016/j.ijpharm.2020.119594.

Awad, A., Yao, A., Trenfield, S.J., Goyanes, A., Gaisford, S., Basit, A.W., 2020b. 3D printed tablets (Printlets) with braille and moon patterns for visually impaired patients. Pharmaceutics 12, 1–14. https://doi.org/10.3390/pharmaceutics12020172.

Basf, 2022. Kollidon VA64 and Kollidon VA64 Fine. Technical Information. Available: https://pharma.basf.com/technicalinformation/30239644/kollidon-va-64-fine.

Berardi, A., Bisharat, L., Quodbach, J., Abdel Rahim, S., Perinelli, D.R., Cespi, M., 2021. Advancing the understanding of the tablet disintegration phenomenon – An update on recent studies. Int. J. Pharm. 598 https://doi.org/10.1016/j.ijpharm.2021.120390.

Blaszczyk, A., Brandt, N., Ashley, J., Tuders, N., Doles, H., Stefanacci, R.G., 2023. Crushed tablet administration for patients with dysphagia and enteral feeding: challenges and considerations. Drugs Aging 40, 895–907. https://doi.org/10.1007/s40266-023-01056-y.

Crișan, A.G., Iurian, S., Porfire, A., Rus, L.M., Bogdan, C., Casian, T., Lucacel, R.C., Turza, A., Porav, S., Tomuță, I., 2022. QbD guided development of immediate release FDM-3D printed tablets with customizable API doses. Int. J. Pharm. 613 https://doi.org/10.1016/j.ijpharm.2021.121411.

de Oliveira, T.V., de Oliveira, R.S., Funk, N.L., Petzhold, C.L., Beck, R.C.R., 2022. Redispersible 3D printed nanomedicines : An original application of the semisolid extrusion technique. Int. J. Pharm. 624, 122029 https://doi.org/10.1016/j.ijpharm.2022.122029.

de Oliveira, R.S., Funk, N.L., dos Santos, J., de Oliveira, T.V., de Oliveira, E.G., Petzhold, C.L., Maria, T., Costa, H., Benvenutti, E.V., Deon, M., Beck, R.C.R., 2023. Bioadhesive 3D-printed skin drug delivery polymeric films : from the drug loading in mesoporous silica to the manufacturing process. Pharmaceutics 15.

Dedroog, S., Pas, T., Vergauwen, B., Huygens, C., Van den Mooter, G., 2020. Solid-state analysis of amorphous solid dispersions: Why DSC and XRPD may not be regarded as stand-alone techniques. J. Pharm. Biomed. Anal. 178, 112937 https://doi.org/10.1016/j.jpba.2019.112937.

dos Santos, J., Souza, G.D., Buchner, S., Mezzomo, F., Windbergs, M., Deon, M., Beck, R.C.R., 2023. 3D printed matrix solid forms : Can the drug solubility and dose customisation affect their controlled release behaviour ? Int. J. Pharm. X 5, 100153. https://doi.org/10.1016/j.ijpx.2022.100153.

El Aita, I., Rahman, J., Breitkreutz, J., Quodbach, J., 2020. 3D-Printing with precise layer-wise dose adjustments for paediatric use via pressure-assisted microsyringe printing. Eur. J. Pharm. Biopharm. 157, 59–65. https://doi.org/10.1016/j.ejpb.2020.09.012.

EuPh, 2019. European Pharmacopeia 10.0: Monographs on dosage forms, Tablets, Dispersible Tablets. Council of Europe, Strasbourg, France.

FDA, 2021. Food and Drug Administration: Oral Drug Products Administered Via Enteral Feeding Tube - In Vitro Testing and Labeling Recommendation, Guidance for Industry. Rockville, MD.

FDA, 2024. Food and Drug Administration: Food and Drugs, Listing of Color Additives Exempt from Certification. Available: https://www.ecfr.gov/current/title-21/chapter-I/subchapter-A/part-73?toc=1.

Fina, F., Goyanes, A., Madla, C.M., Awad, A., Trenfield, S.J., Kuek, J.M., Patel, P., Gaisford, S., Basit, A.W., 2018a. 3D printing of drug-loaded gyroid lattices using selective laser sintering. Int. J. Pharm. 547, 44–52. https://doi.org/10.1016/j.ijpharm.2018.05.044.

Fina, F., Madla, C.M., Goyanes, A., Zhang, J., Gaisford, S., Basit, A.W., 2018b. Fabricating 3D printed orally disintegrating printlets using selective laser sintering. Int. J. Pharm. 541, 101–107. https://doi.org/10.1016/j.ijpharm.2018.02.015.

Funk, N.L., Fantaus, S., Beck, R.C.R., 2022. Immediate release 3D printed oral dosage forms : How different polymers have been explored to reach suitable drug release behaviour. Int. J. Pharm. 625, 122066 https://doi.org/10.1016/j.ijpharm.2022.122066.

Geng, S.T., Zhang, J.B., Wang, Y.X., Xu, Y., Lu, D., Zhang, Z., Gao, J., Wang, K.H., Kuang, Y.Q., 2021. Pre-digested protein enteral nutritional supplementation enhances recovery of CD4+ T Cells and repair of intestinal barrier in HIV-infected immunological non-responders. Front. Immunol. 12, 1–11. https://doi.org/10.3389/fimmu.2021.757935.

Gueche, Y.A., Sanchez-Ballester, N.M., Bataille, B., Aubert, A., Leclercq, L., Rossi, J.C., Soulairol, I., 2021a. Selective laser sintering of solid oral dosage forms with copovidone and paracetamol using a CO2 laser. Pharmaceutics 13, 1–21. https://doi.org/10.3390/pharmaceutics13020160.

Gueche, Y.A., Sanchez-Ballester, N.M., Bataille, B., Aubert, A., Rossi, J.C., Soulairol, I., 2021b. A qbd approach for evaluating the effect of selective laser sintering parameters on printability and properties of solid oral forms. Pharmaceutics 13. https://doi.org/10.3390/pharmaceutics13101701.

Kayalar, C., Helal, N., Mohamed, E.M., Dharani, S., Khuroo, T., Kuttolamadom, M.A., Rahman, Z., Khan, M.A., 2024. In Vitro and In Vivo testing of 3D-Printed Amorphous Lopinavir Printlets by Selective Laser Sinitering: Improved Bioavailability of a Poorly Soluble Drug. AAPS PharmSciTech 25, 1–13. https://doi.org/10.1208/s12249-023-02729-y.

Khuroo, T., Mohamed, E.M., Dharani, S., Kayalar, C., Ozkan, T., Kuttolamadom, M.A., Rahman, Z., Khan, M.A., 2022. Very-rapidly dissolving printlets of isoniazid manufactured by SLS 3D printing. In vitro and in vivo characterization. Mol. Pharm. 19, 2937–2949. https://doi.org/10.1021/acs.molpharmaceut.2c00306.

Kulinowski, P., Malczewski, P., Łaszcz, M., Baran, E., Milanowski, B., Kuprianowicz, M., Dorozynski, P., 2022. Development of Composite, Reinforced, Highly Drug- loaded Pharmaceutical Printlets Manufactured by Selective Laser Sintering—In Search of Relevant Excipients for Pharmaceutical 3D Printing. Materi 2142.

Kulinowski, P., Malczewski, P., Pesta, E., Łaszcz, M., Mendyk, A., Polak, S., Dorożyński, P., 2021. Selective laser sintering (SLS) technique for pharmaceutical applications—Development of high dose controlled release printlets. Addit. Manuf. 38, 101761 https://doi.org/10.1016/j.addma.2020.101761.

Lupone, F., Padovano, E., Casamento, F., Badini, C., 2022. Process phenomena and material properties in selective laser sintering of polymers: A review. Materials (basel). 15 https://doi.org/10.3390/ma15010183.

Madžarević, M., Medarević, Đ., Pavlović, S., Ivković, B., Đuriš, J., Ibrić, S., 2021. Understanding the effect of energy density and formulation factors on the printability and characteristics of SLS Irbesartan tablets—application of the decision tree model. Pharmaceutics 13, 1969. https://doi.org/10.3390/pharmaceutics13111969.

Merck, 2016. Parteck® MXP. Technical Information. Available: https://www.sigmaaldrich.com/deepweb/assets/sigmaaldrich/product/documents/203/518/parteck-mxp-techinfo-141464-mk.pdf.

Merck, 2022. Polyvinyl alcohol for hot melt extrusion. Parteck® MXP: two polymers, unparalleled value. Available: https://www.sigmaaldrich.com/deepweb/assets/sigmaaldrich/product/documents/943/464/parteck-mxp-br9695en-mk.pdf.

Merck, 2023. Candurin Gold Sheen Specification. Available: https://surface-portal.merckgroup.com/BR/en/product/PM/120608.

Mokrane, A., Boutaous, M., Xin, S., 2018. Process of selective laser sintering of polymer powders: Modeling, simulation, and validation. Comptes Rendus Mec. 346, 1087–1103. https://doi.org/10.1016/j.crme.2018.08.002.

Ngilirabanga, J.B., Rosa, P.P., Aucamp, M., Kippie, Y., Samsodien, H., 2020. Dual-drug co-crystal synthesis for synergistic in vitro effect of three key first-line antiretroviral drugs. J. Drug Deliv. Sci. Technol. 60, 101958 https://doi.org/10.1016/j.jddst.2020.101958.

Öblom, H., Sjöholm, E., Rautamo, M., Sandler, N., 2019. Towards printed pediatric medicines in hospital pharmacies: Comparison of 2d and 3d-printed orodispersiblewarfarin films with conventional oral powders in unit dose sachets. Pharmaceutics 11, 1–33. https://doi.org/10.3390/pharmaceutics11070334.

Panraksa, P., Qi, S., Udomsom, S., Tipduangta, P., Rachtanapun, P., Jantanasakulwong, K., Jantrawut, P., 2021. Characterization of hydrophilic polymers as a syringe extrusion 3D printing material for orodispersible film. Polymers (basel). 13 https://doi.org/10.3390/polym13203454.

Rodríguez-Pombo, L., de Castro-López, M.J., Sánchez-Pintos, P., Giraldez-Montero, J.M., Januskaite, P., Duran-Piñeiro, G., Dolores Bóveda, M., Alvarez-Lorenzo, C., Basit, A.W., Goyanes, A., Couce, M.L., 2024. Paediatric clinical study of 3D printed personalised medicines for rare metabolic disorders. Int. J. Pharm. 657, 124140 https://doi.org/10.1016/j.ijpharm.2024.124140.

Rose, A.M., Hall, C.S., Martinez-Alier, N., 2014. Aetiology and management of malnutrition in HIV-positive children. Arch. Dis. Child. 99, 546–551. https://doi.org/10.1136/archdischild-2012-303348.

Seoane-Viaño, I., Xu, X., Ong, J.J., Teyeb, A., Gaisford, S., Campos-Álvarez, A., Stulz, A., Marcuta, C., Kraschew, L., Mohr, W., Basit, A.W., Goyanes, A., 2023. A case study on decentralized manufacturing of 3D printed medicines. Int. J. Pharm. X 5, 100184. https://doi.org/10.1016/j.ijpx.2023.100184.

Seoane-Viaño, I., Pérez-Ramos, T., Liu, J., Januskaite, P., Guerra-Baamonde, E., González-Ramírez, J., Vázquez-Caruncho, M., Basit, A.W., Goyanes, A., 2024. Visualizing disintegration of 3D printed tablets in humans using MRI and comparison with in vitro data. J. Control. Release 365, 348–357. https://doi.org/10.1016/j.jconrel.2023.11.022.

Suárez-González, J., Magariños-Triviño, M., Díaz-Torres, E., Cáceres-Pérez, A.R., Santoveña-Estévez, A., Fariña, J.B., 2021. Individualized orodispersible pediatric dosage forms obtained by molding and semi-solid extrusion by 3D printing: A comparative study for hydrochlorothiazide. J. Drug Deliv. Sci. Technol. 66 https://doi.org/10.1016/j.jddst.2021.102884.

Sustiva, 2023. Product Information - EMEA/H/C/000249 - N/0161. Available: https://www.ema.europa.eu/en/medicines/human/EPAR/sustiva.

Tabriz, A.G., Gonot-Munck, Q., Baudoux, A., Garg, V., Farnish, R., Katsamenis, O.L., Hui, H.-W., Boersen, N., Roberts, S., Jones, J., Douroumis, D., 2023. 3D printing of personalised carvedilol tablets using selective laser sintering. Pharmaceutics 15, 2230. https://doi.org/10.3390/pharmaceutics15092230.

Thakkar, R., Davis, D.A., Williams, R.O., Maniruzzaman, M., 2021a. Selective laser sintering of a photosensitive drug: impact of processing and formulation parameters on degradation, solid state, and quality of 3D-PRINTED DOSAGE FOrms. Mol. Pharm. 18, 3894–3908. https://doi.org/10.1021/acs.molpharmaceut.1c00557.

Thakkar, R., Jara, M.O., Swinnea, S., Pillai, A.R., Maniruzzaman, M., 2021b. Impact of laser speed and drug particle size on selective laser sintering 3d printing of amorphous solid dispersions. Pharmaceutics 13, 1–19. https://doi.org/10.3390/pharmaceutics13081149.

Thakral, N.K., Zanon, R.L., Kelly, R.C., Thakral, S., 2018. Applications of powder X-Ray diffraction in small molecule pharmaceuticals: achievements and aspirations. J. Pharm. Sci. 107, 2969–2982. https://doi.org/10.1016/j.xphs.2018.08.010.

Tikhomirov, E., Åhlén, M., Di Gallo, N., Strømme, M., Kipping, T., Quodbach, J., Lindh, J., 2023. Selective laser sintering additive manufacturing of dosage forms: Effect of powder formulation and process parameters on the physical properties of printed tablets. Int. J. Pharm. 635, 122780 https://doi.org/10.1016/j.ijpharm.2023.122780.

Tranová, T., Pyteraf, J., Kurek, M., Jamróz, W., Brniak, W., Spálovská, D., Loskot, J., Jurkiewicz, K., Grelska, J., Kramarczyk, D., Mužíková, J., Paluch, M., Jachowicz, R., 2022. Fused deposition modeling as a possible approach for the preparation of orodispersible tablets. Pharmaceuticals 15, 69. https://doi.org/10.3390/ph15010069.

Trenfield, S.J., Tan, H.X., Goyanes, A., Wilsdon, D., Rowland, M., Gaisford, S., Basit, A.W., 2020. Non-destructive dose verification of two drugs within 3D printed polyprintlets. Int. J. Pharm. 577 https://doi.org/10.1016/j.ijpharm.2020.119066.

Trenfield, S.J., Xu, X., Goyanes, A., Rowland, M., Wilsdon, D., Gaisford, S., Basit, A.W., 2023. Releasing fast and slow: Non-destructive prediction of density and drug release from SLS 3D printed tablets using NIR spectroscopy. Int. J. Pharm. X 5, 100148. https://doi.org/10.1016/j.ijpx.2022.100148.

USP, 2022. The United States Pharmacopoeia. United States Pharmacopeical Conv.

White, R., Bradnam, V., 2015. Handbook of Drug Administration via Enteral Feeding Tubes, 3rd ed. Pharmaceutical Press.

WHO, 2019. Update of recommendations on first- and second-line antiretroviral regimens. Available: https://iris.who.int/bitstream/handle/10665/325892/WHO-CDS-HIV-19.15-eng.pdf?sequence=1.

WHO, 2023. Epidemiological fact sheet: HIV statistics, globally and by WHO region, 2023. Available: https://www.who.int/teams/global-hiv-hepatitis-and-stis-programmes/hiv/strategic-information/hiv-data-and-statistics.

Windolf, H., Chamberlain, R., Quodbach, J., 2022. Dose-independent drug release from 3D printed oral medicines for patient-specific dosing to improve therapy safety. Int. J. Pharm. 616, 121555 https://doi.org/10.1016/j.ijpharm.2022.121555.